Structure of Mixed-Anions Tris(2-pyridylmethyl)amine Mn Complex, TPAMn(η^2-NO_3)(η-ClO_4)

Bok-Kyu Shin, Mihyang Kim, and Jaehong Han*

*Metalloenzyme Research Group, BET Research Institute and Department of Biotechnology, Chung-Ang University, Anseong 456-756, Korea. *E-mail: jaehongh@cau.ac.kr*

Received December 7, 2006

Mononuclear mixed-anions Mn complex of TPAMn(η^2-NO_3)(η-ClO_4), where TPA is tris(2-pyridylmethyl)-amine, has been synthesized and characterized. The neutral TPAMn(η^2-NO_3)(η-ClO_4) was obtained from the reaction between $Mn(NO_3)_2{\cdot}4H_2O$ and $[H_3TPA](ClO_4)_3$ in MeOH. X-ray crystallographic structure of mononuclear TPAMn(η^2-NO_3)(η-ClO_4) complex showed a seven-coordinated geometry with a tripodal tetradentate TPA, a terminal perchlorate and an η^2-bound nitrate.

Key Words : Mixed-anions, Seven-coordinated manganese complex, Tripodal ligand, Crystal structure, Nitrate binding

Introduction

Manganese centers play important roles in biological system and various nuclearities of Mn cores are found in the active sites of the enzymes.[1] For examples, manganese catalase contains a dinuclear Mn center in the active site, and catalyzes dismutation of hydrogen peroxide into water and oxygen molecules.[2] Arginase with a similar dinuclear Mn active center shows an activity of arginine hydrolysis to the ornithine and urea.[3] Oxygen-evolving complex of photosystem II contains tetranuclear manganese cluster for water oxidation.[4,5] There are also many enzymes with mononuclear manganese active center, manganese superoxide dismutase, manganese peroxidase, and relatively unknown integrase. Manganese-superoxide dismutase has a mononuclear manganese center with trigonal bipyramidal coordination geometry and detoxifies reactive oxygen species.[6,7] Manganese peroxidase involved in lignin degradation oxidizes octahedral Mn(II) ion to form the Mn(III)-organic acid complexes.[8] Integrase, involved in the retroviral replication cycle of human immunodeficiency virus, has a mononuclear manganese center with octahedral coordination geometry.[9] These manganese centers interact with various ligands for their activities, including oxo, hydroxo, water, superoxide anion, hydrogen peroxide and molecular oxygen. Such versatile ligand binding, coordination geometries, and catalytic activities of Mn complexes are of a great interest.[10,11]

Due to the easy preparation and versatile coordination chemistry, TPA (tris(2-pyridylmethyl)amine) has been used as a popular biomimetic ligand. Various alkali metal and transition metal complexes of TPA were synthesized and used for biological model systems, such as dioxygen activation by iron non-heme oxygenases.[12] Although many TPA manganese complexes have been reported,[13-16] the complexes with weak anionic terminal ligands are rare.[17] Especially, the complex with mixed-anionic terminal ligands has never been reported to our knowledge. Here we report the synthesis and X-ray crystallographic structure of the TPAMn(η^2-NO_3)(η-ClO_4) complex. The catalytic activity of hydrogen peroxide dismutation of the TPAMn(η^2-NO_3)(η-ClO_4) complex also has been carried out.

Experimental

General. All experiments and reactions were carried out under air. All solvents were purified using standard methods before each use.[18] $Mn(NO_3)_2{\cdot}4H_2O$ was purchased from Aldrich and used without further purification. $H_3TPA(ClO_4)_3$ was prepared from the published method.[19] FT-IR spectra were collected on a Nicolet DX V. 4.56 FT-IR spectrometer in KBr pellets and the spectra were corrected for background. Elemental analyses were performed in the Microanalytical Laboratory at the University of Michigan. The data were corrected using acetanilide as a standard.

Catalytic study. In 20 mL vial with a stirring bar, Mn complex was dissolved in 3.0 mL of MeCN under dinitrogen to make 0.1 mM solution. The vial was sealed with septum, and connected to the gas volume measurement apparatus through double-ended needle. The catalysis was initiated by introducing 18% H_2O_2 solution using syringe. The amount of product formation was calculated from the volume of oxygen gas generated using the ideal-gas equation. The substrate concentration vs. initial velocity graph was obtained from four independent measurements at each substrate concentration.

TPAMn(η^2-NO_3)(η-ClO_4). $Mn(NO_3)_2{\cdot}4H_2O$ (0.15 g, 0.6 mmol) in MeOH (2 mL) was added to 3 mL of methanol solution of $H_3TPA(ClO_4)_3$ (0.355 g, 0.6 mmol) and NEt_3 (0.251 mL, 1.8 mmol). The reaction mixture was stirred for two hours at room temperature. Diethyl ether was added into the reaction mixture and yellow oil was formed in a few days. The solvent was removed by decanting and the oil was dried under vacuum. It was redissolved in 3 mL of MeOH and solvent diffusion by the ethyl ether produced transparent crystals in a day. TPAMn(η^2-NO_3)(η-ClO_4) (150 mg, 0.295 mmol, 49%). FT-IR (KBr, cm^{-1}) $\nu(C_{Ar}$-H): 3079(w), ν(C-

H); 2862(w), ν(C=N); 1609(s), $\nu(NO_3)$; 1483(m), 1467(s), and 817(w), $\nu(ClO_4)$; 1118(s) and 1102(vs). Anal. Calcd for $C_{18}H_{18}ClMnN_5O_7$ (MW 506.756): C, 42.66; H, 3.58; N, 13.82. Found: C, 42.62; H, 3.56; N, 13.76.

X-ray Crystallography. Transparent irregular-shaped crystals of TPAMn(η^2-NO_3)(η-ClO_4) were obtained from the mother liquor by solvent diffusion after several days. The diffraction data was collected at 123(2) K using a Bruker SMART area diffractometer equipped with a monochromator in the Mo Kα (λ = 0.71073 Å) incident beam. The CCD data were integrated and scaled using the Bruker-SAINT software package,[20] and the structure was solved and refined using SHEXTL V5.10.[21] The crystal data and structural parameters are shown in Tables 1 and Table 2. The structure was solved by direct methods to locate heavy atoms, and the nonhydrogen atoms were located through subsequent difference Fourier syntheses. Structural refinement was carried out by full-matrix least squares on F^2. All non-hydrogen atoms were refined with anisotropic thermal parameters. Hydrogen atoms were located in the calculated positions.

Results and Discussion

The similar TPAMn(η^2-NO_3)(η-NO_3) complex was synthesized from the reaction between TPA and $Mn(NO_3)_2{\cdot}4H_2O$ in MeOH.[17] By substituting TPA with $H_3TPA(ClO_4)_3$, mixed-anions TPAMn(η^2-NO_3)(η-ClO_4) was achieved. The nitrate group at 1483 cm^{-1}, 1467 cm^{-1} and 817 cm^{-1}, and the perchlorate group at 1118 cm^{-1} and 1102 cm^{-1} were observed from IR spectrum. It appears formation of the complex is favored in the presence of perchlorate ion during the reaction or crystallization process.

Solid state structure of TPAMn(η^2-NO_3)(η-ClO_4) complex has been characterized by single crystal X-ray crystallography at 123(2) K. It was crystallized in the monoclinic $P2_1/c$ space group (Table 1). The neutral Mn complex is a seven-coordinate Mn(II) complex with two terminally bound η^2-nitrate and η-perchlorate anions (Figure 1, Table 2). The

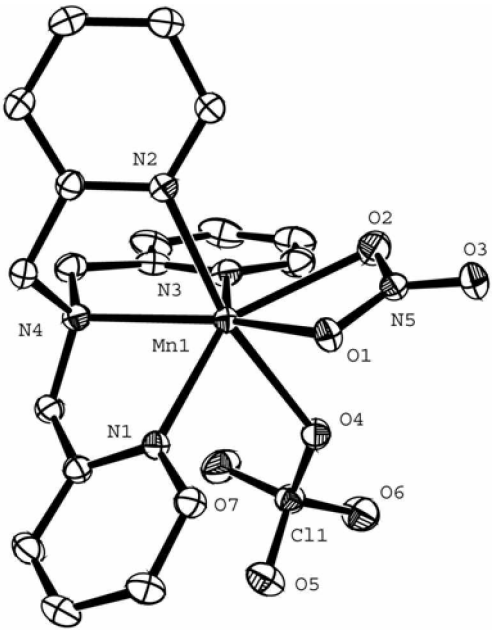

Figure 1. Crystallographic structure of TPAMn(η^2-NO_3)(η-ClO_4) with thermal ellipsoids (50% probability); hydrogen atoms omitted for clarity.

Table 1. Crystal data and structure refinement for TPAMn(η^2-NO_3)(η-ClO_4)

Empirical formula	$C_{18}H_{18}ClMnN_5O_7$
Formula weight	506.76
Temperature	123(2) K
Wavelength	0.71073 Å
Crystal system, space group	Monoclinic, $P2_1/c$
Unit cell dimensions	a = 14.140(4) Å
	b = 9.161(3) Å
	c = 16.082(5) Å
	β = 90.795(5)°
Volume	2083.1(11) $Å^3$
Z, Calculated density	4, 1.616 Mg/m^3
Absorption coefficient	0.815 mm^{-1}
F(000)	1036
Crystal size	0.48 × 0.44 × 0.44 mm
θ range for data collection	2.53 to 28.33°
Limiting indices	$-18 \le h \le 18$
	$-12 \le k \le 12$
	$-21 \le l \le 21$
Reflections collected / unique	45087 / 5176
R(int)	0.0290
Completeness to theta	28.33°, 99.4%
Absorption correction	Semi-empirical
Refinement method	Full-matrix least-squares on F^2
Data / restraints / parameters	5176 / 0 / 361
Goodness-of-fit on F^2	1.041
Final R indices [I > 2sigma(I)]	R1 = 0.0262, wR2 = 0.0767
R indices (all data)	R1 = 0.0285, wR2 = 0.0780
Largest diff. peak and hole	0.371 and −0.700 $e.Å^{-3}$

Table 2. Selected bond lengths [Å] and angles [°] for TPAMn(η^2-NO_3)(η-ClO_4)

Mn(1)-N(1)	2.2538(12)	N(3)-Mn(1)-N(1)	129.17(4)
Mn(1)-N(2)	2.2680(13)	N(3)-Mn(1)-O(1)	138.79(4)
Mn(1)-N(3)	2.2288(13)	N(1)-Mn(1)-O(1)	85.23(4)
Mn(1)-N(4)	2.3559(12)	N(3)-Mn(1)-N(2)	92.82(4)
Mn(1)-O(1)	2.2573(12)	N(1)-Mn(1)-N(2)	111.50(4)
Mn(1)-O(2)	2.4290(12)	O(1)-Mn(1)-N(2)	93.77(4)
Mn(1)-O(4)	2.4071(11)	N(3)-Mn(1)-N(4)	74.39(5)
Cl(1)-O(4)	1.4718(10)	N(1)-Mn(1)-N(4)	71.91(4)
Cl(1)-O(5)	1.4409(11)	O(1)-Mn(1)-N(4)	145.80(4)
Cl(1)-O(6)	1.4267(12)	N(2)-Mn(1)-N(4)	72.48(4)
Cl(1)-O(7)	1.4293(12)	N(3)-Mn(1)-O(4)	82.38(4)
O(1)-N(5)	1.2731(15)	N(1)-Mn(1)-O(4)	80.01(4)
O(2)-N(5)	1.2656(16)	O(1)-Mn(1)-O(4)	82.71(4)
O(3)-N(5)	1.2296(15)	N(2)-Mn(1)-O(4)	167.74(4)
O(1)-N(5)-O(2)	116.53(11)	N(4)-Mn(1)-O(4)	116.57(4)
O(1)-N(5)-O(3)	121.06(12)	N(3)-Mn(1)-O(2)	84.94(5)
O(2)-N(5)-O(3)	122.40(11)	N(1)-Mn(1)-O(2)	137.11(4)
O(5)-Cl(1)-O(6)	109.32(7)	O(1)-Mn(1)-O(2)	54.72(4)
O(4)-Cl(1)-O(5)	109.70(6)	N(2)-Mn(1)-O(2)	88.14(4)
O(4)-Cl(1)-O(6)	108.14(6)	N(4)-Mn(1)-O(2)	150.55(4)
O(4)-Cl(1)-O(7)	108.75(7)	O(4)-Mn(1)-O(2)	80.23(4)

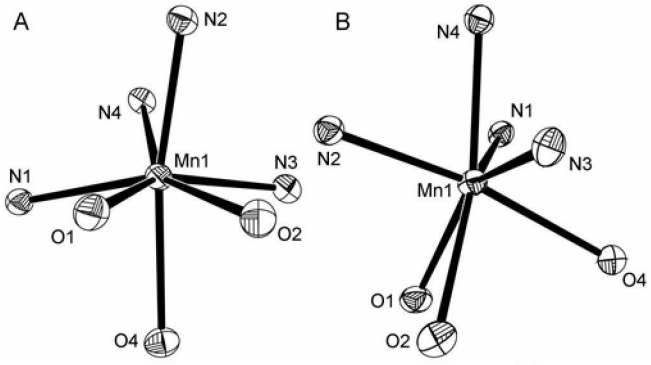

Figure 2. The two possible coordination geometries for the seven-coordinate TPAMn(η^2-NO$_3$)(η-ClO$_4$) complex: A, pentagonal bipyramid; B, capped octahedron.

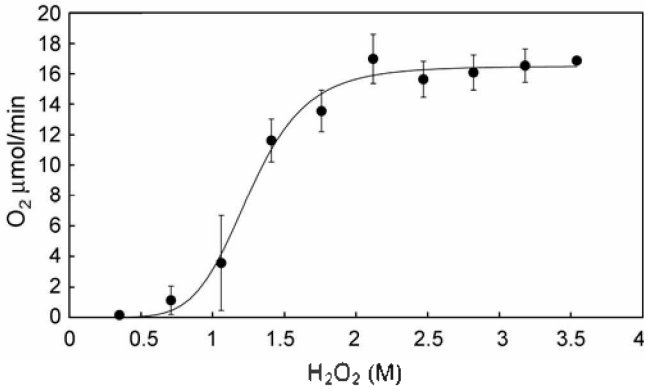

Figure 3. Reaction rate of O_2 generation by the TPAMn(η^2-NO$_3$)(η-ClO$_4$) complex. The bars represent ranges of experimental data. The data were simulated with Hill equation and represented as a solid line.

coordination geometry around Mn atom can be considered as a distorted pentagonal bipyramid or a distorted capped octahedron (Figure 2). For the pentagonal bipyramidal coordination geometry (Figure 2A), the N(2) and O(4) atoms form axial ligands. The other five atoms are bound to Mn center as pentagonal equatorial ligands. The distances of Mn(1)-N(2) and Mn(1)-O(4) bonds are found at 2.2680(13) Å and 2.4071(11) Å, respectively. The axial angle between these two ligands is 167.74(4)° and distorted from the ideal 180°. The N(4) atom becomes the axial ligand of the distorted capped octahedral coordination geometry, while the other six atoms form the octahedron (Figure 2B). Two N(1)-N(2)-N(3) and O(1)-O(2)-O(4) trigonal planes form the base of octahedron. These possible two coordination geometries show easy interconversions of seven-coordinated complexes.[22]

TPA ligand is bound to the Mn(1) in a tetradentate mode, with bond distances of 2.2538(12) Å, 2.2680(13) Å, 2.2288 (13) Å and 2.3559(12) Å for Mn(1)-N(1), Mn(1)-N(2), Mn(1)-N(3), and Mn(1)-N(4), respectively. The average Mn-N distance[23] of 2.277(14) Å implies a possible high spin configuration of the TPAMn(η^2-NO$_3$)(η-ClO$_4$) complex.[24] The nitrate group is bound to Mn(1) atom in η^2-fashion with distances of 2.2573(12) Å and 2.4290(12) Å for Mn(1)-O(1) and Mn(1)-O(2), respectively. The difference between these two distances is 0.1717 Å (parameter *a*). The distance of Mn(1)-N(5) is found at 2.745 Å and the difference between Mn(1)-N(5) and Mn(1)-O(2) is 0.316 Å (parameter *b*). The angles of Mn(1)-O(1)-N(5) and Mn(1)-O(2)-N(5) are found at 98.19(8)° and 90.31(7)°, respectively, and the difference is 7.88° (parameter *c*). Anisobidentate and bidentate mode are possible for the η^2-nitrate and these parameters are the criteria to determine the binding mode of nitrate ligand.[25] Parameter *a* is smaller than 0.3 Å, parameter *b* is greater than 0.2 Å, and parameter *c* is smaller than 14°. Accordingly, binding mode of nitrate ligand was assigned to bidentate. The perchlorate group is bound to the Mn(1) center in an η-geometry.

The O_2 formation by the TPAMn(η^2-NO$_3$)(η-ClO$_4$) complex was measured by the O_2 gas volume. The complex dismutated hydrogen peroxide catalytically. The substrate vs. initial velocity plot is shown at Figure 3. Because the catalysis followed sigmoidal kinetics, the plot was fitted with Hill equation.[26] Sigmoidal kinetics is usually observed from the multi-subunit enzyme catalysis or from the substrate-dependent enzyme activation.[27] In case of the TPAMn (η^2-NO$_3$)(η-ClO$_4$) complexes, substrate-activation of the catalyst seems to be the reason for the observed sigmoidal kinetics. Its K_M and k_{cat} are 1.26 ± 0.03 M and 0.92 ± 0.02 s^{-1}, respectively, with Hill constant of 6.3 ± 0.9. The active Mn catalase was reported to show 260000 s^{-1} of k_{cat}.[28] It is highly likely that the anionic terminal ligands can be dissociated from the Mn center during the catalysis, and which allows H_2O_2 binding to the Mn center. Currently, it is not clear whether the complex goes through dimerization to form the Mn catalase-like catalyst. The reaction velocity was linearly dependent on the concentration of the complex. It indicates the dimerization step, even it does occur, is not a rate limiting step for the catalysis.

In summary, the TPAMn(η^2-NO$_3$)(η-ClO$_4$) complex has been synthesized and structurally characterized. The complex was characterized as a high spin d^5 complex based on the structural parameters. Catalytic study suggested the nitrate and perchlorate ligands are labile under the catalytic conditions.

Acknowledgment. This work was supported by the Korean Research Foundation Grant (KRF-2006-331-F00015) funded by the Korean Government (MOEHRD).

Supplementary data. Crystallographic data for the structure reported here have been deposited with Cambridge Crystallographic Data Center (Deposition No. CCDC 629936). The data can be obtained free of charge *via* www.ccdc.cam.ac.uk/conts/retrieving.html (or from the CCDC, 12 Union Road, Cambridge CB2 1EZ, UK; fax: +44 1223 336033; e-mail: deposit@ccdc.cam.ac.uk).

References

1. Horsburgh, M. J.; Wharton, S. J.; Karavolos, M.; Foster, S. J.

Trends Microbiol. **2002**, *10*, 496.
2. Whittaker, M. M.; Barynin, V. V.; Antonyuk, S. V.; Whittaker, J. W. *Biochemistry* **1999**, *38*, 9126.
3. Kanyo, Z. F.; Scolnick, L. R.; Ash, D. E.; Christianson, D. W. *Nature* **383**, 554.
4. Balsera, M.; Arellano, J. B.; Revuelta, J. L.; Rivas, J.; Hermoso, J. A. *J. Mol. Biol.* **2005**, *350*, 1051.
5. Ferreira, K. N.; Iverson, T. M.; Maghlaoui, K.; Barber, J.; Iwata, S. *Science* **2004**, *303*, 1831.
6. Dennis, R. J.; Micossi, E.; McCarthy, J.; Moe, E.; Gordon, E. J.; Kozielski-Stuhrmann, S.; Leonard, G. A.; McSweeney, S. *Acta Cryst. F* **2006**, *62*, 325.
7. Atzenhofer, W.; Regelsberger, G.; Jacob, U.; Peschek, G. A.; Furtmüller, P. G.; Huber, R.; Obinger, C. *J. Mol. Biol.* **2002**, *321*, 479.
8. Sundaramoorthy, M.; Youngs, H. L.; Gold, M. H.; Poulos, T. L. *Biochemistry* **2005**, *44*, 6463.
9. Bujacz, G.; Jaskolski, M.; Alexandratos, J.; Wlodawer, A.; Merkel, G.; Katz, R. A.; Skalka, A. M. *Structure* **1996**, *4*, 89.
10. Liu, Z.-X.; Cho, M.-W.; Baeg, J.-O.; Lee, C. W. *Bull. Korean Chem. Soc.* **2006**, *27*, 2064.
11. Baik, J. S.; Lee, N. H. *Bull. Korean Chem. Soc.* **2006**, *27*, 765.
12. Canary, J. W.; Wang, Y.; Roy, Jr., R. *Inorg. Synth.* **1998**, *32*, 70.
13. Towle, D. K.; Botsford, C. A.; Hodgson, D. J. *Inorg. Chim. Acta* **1988**, *141*, 167.
14. Xiang, D. F.; Duan, C. Y.; Tan, X. S.; Liu, Y. L.; Tang, W. X. *Polyhedron* **1998**, *17*, 2647.
15. Oshio, H.; Ino, E.; Mogi, I.; Ito, T. *Inorg. Chem.* **1993**, *32*, 5697.
16. Gultneh, Y.; Farooq, A.; Karlin, K. D.; Liu, S.; Zubieta, J. *Inorg. Chim. Acta* **1993**, *211*, 171.
17. Baldeau, S. M.; Slinn, C. H.; Krebs, B.; Rompel, A. *Inorg. Chim. Acta* **2004**, *357*, 3295.
18. Perrin, D. D.; Armarego, W. L. F. *Purification of Laboratory Chemicals*, 3rd ed.; Pergamon: New York, 1988.
19. Mandel, J. B.; Maricondi, C.; Douglas, B. E. *Inorg. Chem.* **1988**, *27*, 2990.
20. Bruker *SMART and SAINT*; Bruker AXS Inc.: Madison, Wisconsin, USA, 1997.
21. Bruker *SHELATL*, Version 5.10; Bruker AXS Inc.: Madison, Wisconsin, USA, 1998.
22. Cotton, F. A.; Wilkinson, G.; Murillo, C. A.; Bochmann, M. In *Advanced Inorganic Chemistry*, 6th ed.; Wiley-Interscience: New York, 1999; p 7.
23. The number in the parenthesis of average bond distances represents the larger of the individual standard deviations or the standard deviation from the mean. σ = SQRT[$\Sigma_{i=1}^{n}(x_i-x)^2/n(n-1)$], where x_i is an individual standard deviation, x is the average of individual standard deviations.
24. Zang, Y.; Kim, J.; Dong, Y.; Wilkinson, E. C.; Appelman, E. H.; Que, L., Jr. *J. Am. Chem. Soc.* **1997**, *119*, 4197.
25. Kleywegt, G. J.; Wiesmeijer, W. G. R.; Van Driel, G. J.; Driessen, W. L.; Reedijk, J.; Noordik, J. H. *Dalton Trans.* **1985**, 2177.
26. Hill equation, $v_i = V_{max}[H_2O_2]^n/(K_M^n + [H_2O_2]^n)$, where v_i: initial velocity, V_{max}: maximum velocity, $[H_2O_2]$: concentration of substrate, n: Hill constant, K_M: Michaelis constant.
27. Kuby, S. A. *A Study of Enzymes*, Vol. 1; CRC Press: Florida, 1991.
28. Shank, M.; Barynin, V.; Dismukes, G. C. *Biochemistry* **1994**, *33*, 15433.